Dissipative effects on quarkonium spectral functions

Yusuf Buyukdag[1,*] and Clint Young[1,†]

[1]*School of Physics & Astronomy, University of Minnesota, Minneapolis, MN 55455,USA*

(Dated: April 2, 2015)

Abstract

Quarkonium at finite temperature is described as an open quantum system whose dynamics are determined by a potential $V_R(\mathbf{x})$ and drag coefficient η, using a path integral with a non-local term. Path-integral Monte Carlo calculations determine the Euclidean Green function for this system to an accuracy greater than one part in a thousand and the maximum entropy method is used to determine the spectral function; challenges facing any kind of deconvolution are discussed in detail with the aim of developing intuition for when deconvolution is possible. Significant changes to the quarkonium spectral function in the $1S$ channel are found, suggesting that any description of quarkonium at finite temperature, using a potential, must also carefully consider the effect of dissipation.

*Electronic address: buyuk007@umn.edu

†Electronic address: young@physics.umn.edu

I. INTRODUCTION

At both zero temperature and above deconfinement, quarkonium is an ideal probe of QCD. At zero temperature its mass $M \gg \Lambda_{\rm QCD}$ suggests the effective field theory approach of NRQCD [1], where the heavy quark mass is integrated out. In effect, the heavy quark mass sets the momentum scale of QCD for states using this description, allowing perturbative results to work well. The situation becomes more complicated at finite temperatures. NRQCD can be extended to finite temperature and used to examine the break-up of quarkonium [2].

An alternative point of entry is to treat quarkonium above deconfinement as an open quantum system (OQS)[4]. This departs from any attempt to describe quarkonium with perturbation theory, and the parameters describing quarkonium have to be determined separately, either in calculations based on first principles or from experimental measurements. However, this description has the strength of being independent of some of the scale hierarchies. One would suspect that the OQS approach is at its most useful for charmonium and highly excited states of bottomonium, where the binding energy is small and the confining term of the Cornell potential is important for describing the spectrum of states at zero temperature. Perhaps the greatest strength of the OQS approach is that the approach to thermalized yields of quarkonium is completely natural, which is not necessarily the case for some potential models. Since the first, simplest descriptions of quarkonium in this way, the treatment of heavy quarks at finite temperature has developed significantly, thanks the work of several authors [5–7].

This paper describes the numerical determination of the spectral function for an open quantum system, which has the potential term and the diffusion coefficient matched to quarkonium at the temperatures reached in heavy-ion collisions. The procedures used can be generalized for different densities of states for the thermal bath, for different couplings, and for non-trivial correlations of the bath's force on the heavy quark and the anti-quark. In Section II, the path-integral Monte Carlo algorithm for this open quantum system is described. In Section III, intuition is developed for when phenomenologically significant deconvolution of spectral functions is possible, with this having some implications for results using lattice QCD calculations; and finally, the maximum entropy method is used to deconvolve the results from Section II into quarkonium spectral functions, and the non-trivial relationship between diffusion and the destruction of the J/ψ state can be determined. In

this way, the often competing effects of drag and momentum diffusion on J/ψ survival rates can be simultaneously considered, as was done in [8, 9].

While this procedure may seem cumbersome, it is in fact relatively cheap computationally. The most costly step is the calculation of the correlation functions to sufficient accuracy so that deconvolution yields significant results; work on high-order estimates of the action in Equation 4 can speed this computation significantly as it has for simple actions.

II. EUCLIDEAN CURRENT-CURRENT CORRELATORS AND DISSIPATIVE EFFECTS

Much of the groundwork towards examining open quantum systems with path integrals was already done by Feynman and Hibbs when they considered influence functionals [10]; Caldeira and Leggett used path integrals to describe a system with a specific thermal bath [11] while Grabert, Schramm, and Ingold generalized Caldeira and Leggett's results [12]. In [4], these techniques were applied to imaginary-time Green functions. To review: one starts with the action for a heavy degree of freedom with position x interacting with a light degree of freedom described by R. This light degree of freedom is often a collective mode of a gas or of condensed matter, and not just a value for position. The action for this system, using a harmonic approximation and minimal coupling, is

$$S = \int_0^\tau d\tau^{'} \left[\frac{1}{2}M\dot{x}^2 + V(x) + \frac{1}{2}m\dot{R}^2 + \frac{1}{2}m\omega^2 R^2 - CxR\right]$$

gives the influence functional

$$\begin{aligned}\langle x_f, \tau | x_i, 0\rangle_{\text{red}} = \int \mathcal{D}x \ \exp\Bigg(-\int_0^\tau d\tau^{'} \Bigg[\frac{1}{2}M\dot{x}^2 + V(x) \\ -\frac{C^2}{2m\omega\sinh(\omega\tau)}x(\tau^{'})\cosh(\omega(\tau-\tau^{'}))\int_0^{\tau^{'}} ds\ x(s)\cosh(\omega s)\Bigg]\Bigg). \qquad (1)\end{aligned}$$

after finding $\langle x_f, R_f | x_i, R_i\rangle$ and integrating over R_i and R_f. When there are multiple light degrees of freedom, the final term in the integral becomes the sum $\sum_i \frac{C_i^2}{2m_i\omega_i\sinh(\omega_i\tau)}x(\tau^{'})\cosh(\omega_i(\tau-\tau^{'}))\int_0^{\tau^{'}} ds\ x(s)\cosh(\omega_i s)$. The system becomes dissipative in the limit of an infinite number of light degrees of freedom of masses m_i and frequencies

ω_i: the density of states

$$C^2(\omega)\rho_D(\omega) = \begin{cases} \frac{2m\eta\omega^2}{\pi} & \text{if } \omega < \Omega \\ 0 & \text{if } \omega > \Omega \end{cases} \tag{2}$$

in the limit $\Omega \to \infty$ was examined in [11] and found to lead to a path integral which yields the Langevin equation in the classical, high-temperature limit. Performing the integral over these states in Equation 1 leads to the integral

$$\begin{aligned} &\int_0^\Omega d\omega \int_0^\tau du \int_0^\tau dv\ x(u)x(v)\frac{\omega\cosh(\omega(\tau-u))\cosh(\omega v)}{\sinh(\omega\tau)}\theta(u-v) \\ &= \frac{\Omega}{2}\int_0^\tau du(x(u))^2 - \int_0^\Omega \frac{d\omega}{\omega\sinh(\omega\tau)}\int_0^\tau du\int_0^u dv\ \dot{x}(u)\dot{x}(v)\sinh(\omega(\tau-u))\sinh(\omega v), \end{aligned}$$

which forces a renormalization of $V(x)$, and gives the imaginary-time Green function for this system:

$$G_{\rm red}(x_f, x_i, \tau) = \int \mathcal{D}x\ \exp\left(-\int_0^\tau du\left[\frac{1}{2}M\dot{x}(u)^2 + V_R(x(u)) - \frac{\eta}{2\pi}\int_0^u dv\ \dot{x}(u)\dot{x}(v)\log\left[\frac{\sin(\frac{\pi}{2}\frac{u-v}{\tau})}{\sin(\frac{\pi}{2}\frac{u+v}{\tau})}\right]\right]\right).$$

Note that only the potential is renormalized, and that the final term introduced by the integration over the bath of particles is translationally invariant, meaning that no finite, x-dependent term has been added to the path integral. This imaginary-time Green function can be made periodic in τ with period β using the method of images to make a quantity related to results from finite-temperature lattice calculations.

For a general potential, numerical methods for determining this path integral must be developed. Path-integral Monte Carlo techniques have been developed for condensed matter systems; Ceperley reviewed these methods as they concern liquid helium [13]. For quarkonium, a relatively simple algorithm is used: the path is discretized to $2^{11}+1$ equally-spaced times, and free-particle paths are sampled using the bisection method. These paths are reweighted according to the expression above. The double integral in the exponential poses some problems because it is improper; both the "square" and "triangular" regions in the double integral must have their measures determined analytically so that sufficient precision may be achieved.

The results for $G(\tau)$ have been calculated for the Cornell-like potential

$$V(r) = \begin{cases} -\frac{1.5\alpha_s}{r_{\min}} + 0.5\sigma r_{\min} + (\frac{0.5\alpha_s}{r_{\min}} + 0.5\sigma r_{\min})\frac{r^2}{r_{\min}^2} \\ \text{if } r < r_{\min}, \\ -\alpha_s/r + \sigma r \text{ if } r > r_{\min} \end{cases} \tag{3}$$

with $r_{\min}$ chosen to be small, 0.4 GeV^{-1} (here, all units are in GeV), $\alpha_s = 0.499$, and $\sigma = 0.16$ GeV^2. The purpose of using this piecewise function is to simplify dealing with the divergence of the Cornell potential as $r \to 0$. The drag coefficients η =0, 0.0729 GeV, and 0.1458 GeV were used, corresponding to the spatial diffusion coefficients $2\pi D_c = \infty$, 5, and 2.5, respectively, at $T = 285$ MeV. The results for these values were shown in [4]; here, in Figure 1, we show results for the same values but for a large range in τ, which is necessary for extracting the spectral function. We should also note that some degrees of freedom of the heavy quark are not represented in this path integral, namely, spin and color. The potential term is therefore the thermal average of this quantity over spin and color states. In [6], Lindblad equations describing the evolution of color singlet and octet states are determined for heavy quarkonium, starting from perturbative QCD for heavy quarks. Our path integral, on the other hand, requires color-averaged potentials as an input for the path integral Monte Carlo calculations.

III. THE QUARKONIUM SPECTRAL FUNCTION AND THE CHALLENGES FACING DECONVOLUTION

The imaginary-time Green function is related to the spectral function $\rho = -\text{Im}\{G_R\}$ through a Laplace transform:

$$G(\tau) = \int \exp(-\omega\tau)\rho(\omega)d\omega; \tag{4}$$

similarly, the imaginary-time finite-temperature Green function is this Laplace transform made periodic through the method of images:

$$G(\tau, \beta) = \int \frac{\cosh(\omega(\tau - \beta/2))}{\sinh(\omega\beta/2)}\rho(\omega)d\omega. \tag{5}$$

Complex analysis helps here: the Fourier transforms of the various Green functions are conveniently related to each other; as a function of complex ω, causality translates to analyticity

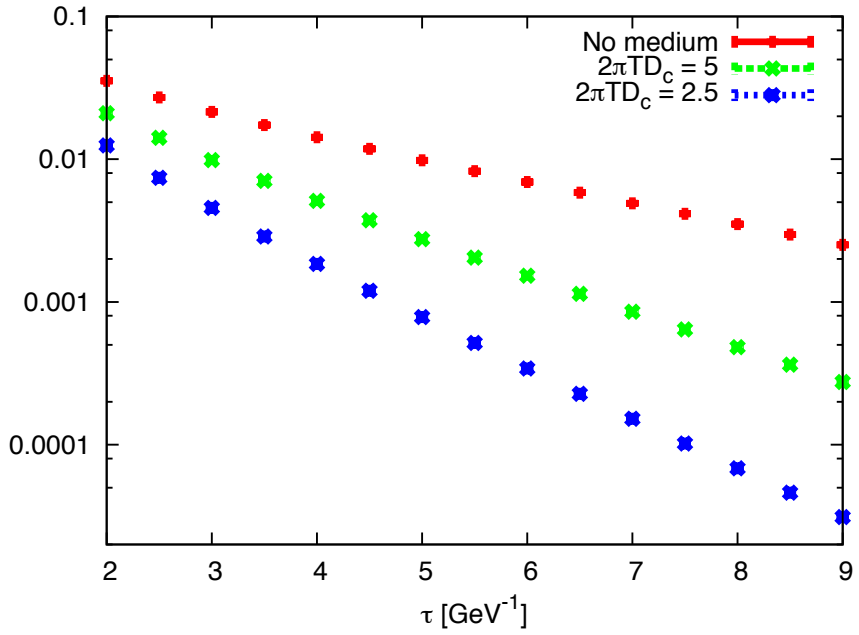

FIG. 1 (Color Online): From [4], $G(\tau)$ with and without dissipative effects.

of G_R in the upper-half plane; and the relation between G_R and G_A in ω is a generalization of the fluctuation-dissipation theorem [14].

Unfortunately, when working with numerical results and not analytic expressions for $G(\tau)$, these results are not helpful. The reason for this is simple: significantly different spectral functions often differ by very little in their Laplace transforms. This is not obvious to theorists who work with analytic results so it is necessary to illustrate this with an example: consider two spectral functions, ρ_1 and ρ_2, plotted in Figure 2. The widths differ by a factor of five, from 0.01 GeV for ρ_1 to 0.05 GeV for ρ_2. This changes the lifetime of the state from $\sim$ 20 fm/c to $\sim$ 4 fm/c. The lifetime of the state represented by ρ_1 is long compared with the timescales of the heavy-ion collisions at RHIC and the LHC; it represents a state whose yields would be largely unaffected, while the state represented by ρ_2 would be significantly suppressed.

Lattice QCD calculations of quarkonium correlation functions have determined $G(\tau, \beta)$ for temperatures between $T_c = 175$ MeV and $2T_c$, by determining the correlation functions of composite operators

$$G(\tau, \beta) = \int d^3x \, \langle J_\mu(\mathbf{x}, \tau) J^\mu(\mathbf{x}, \tau) \rangle \, , \tag{6}$$

where $J_\mu = \bar{\psi} \Gamma_\mu \psi$ and $\Gamma_\mu = \gamma_\mu, \, \gamma_4 \gamma_\mu$. This function corresponds to the transform of the

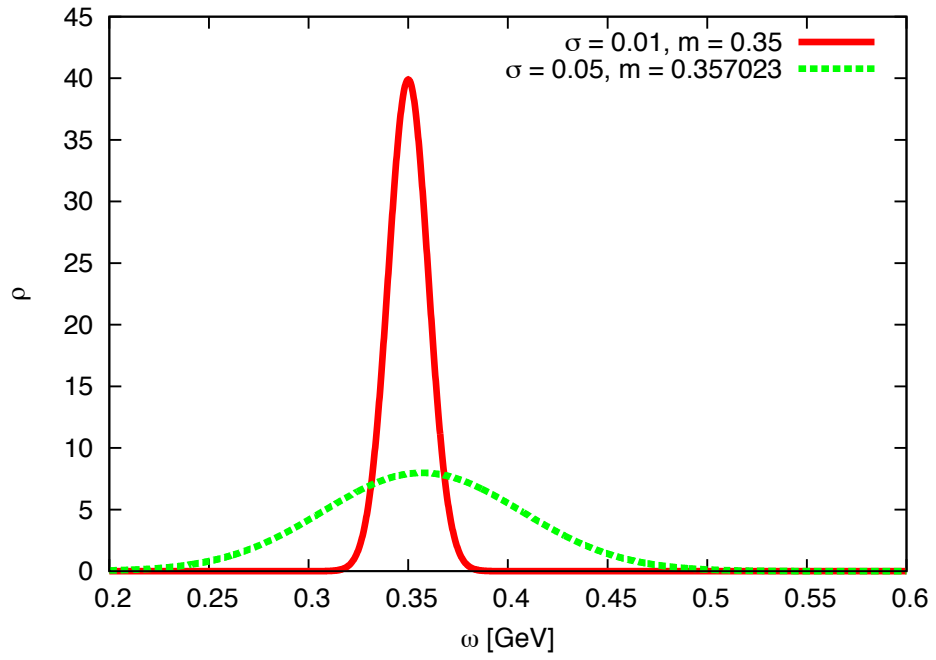

FIG. 2 (Color Online): The spectral functions ρ_1 (with width $\sigma = 0.01$ GeV) and ρ_2 (with width $\sigma = 0.05$ GeV).

spectral function shown in Equation 5. For $\beta = (1.5T_c)^{-1}$, this transform of ρ_1 and ρ_2 can be computed; Figure 3 shows the relative difference $\Delta G/G \equiv (G_2 - G_1)/G_2$ for values of τ from zero to 0.5β.

The relative difference has a maximum of about one part in a thousand. If the full range for τ were equally sensitive to changes in this bound state, this would suggest that three results for $G(\tau, \beta)$, equally spaced on this range, would need an accuracy of a few parts in ten thousand to determine which spectral function fits the results best. Constraining the spectral function in the vector channel with sum rules is not likely to help much because they provide only a few constraints to a continuous function.

Lattice QCD calculations at specific temperatures are performed on periodic lattices and are used to determine finite-temperature Green functions as in Equation 5, not 4. However, if another calculation can determine imaginary-time Green functions as in Equation 4 at large τ, it will be sensitive mostly on the shape of the ground state and the resulting G_1 and G_2 should differ by a greater relative ΔG. We take advantage of this fact by calculating this Green function for a dissipative system over the range shown in Figure 4. Here, $|\Delta G|/G$ has a maximum of about 1%, suggesting that numerical deconvolution will be less daunting.

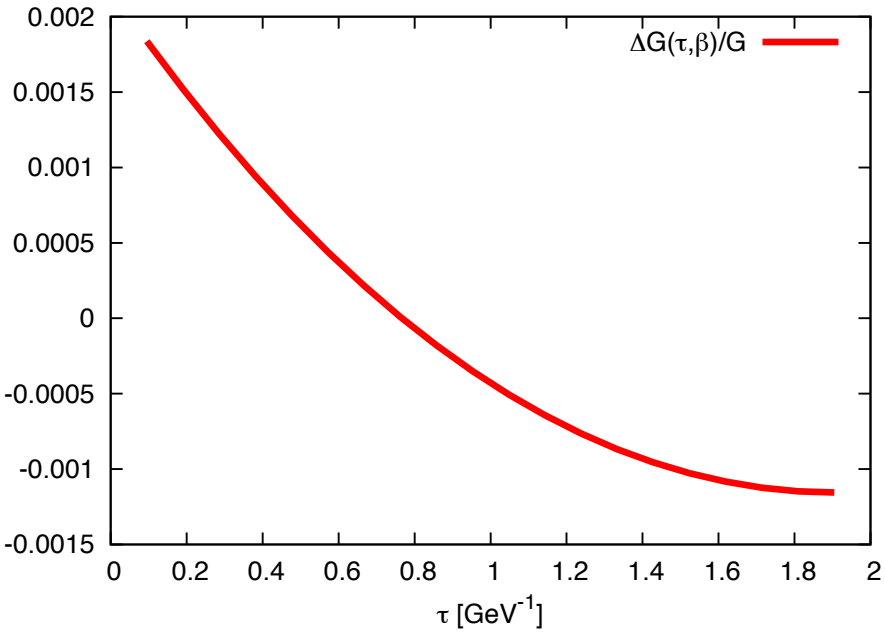

FIG. 3 (Color Online): The relative difference $\Delta G/G = (G_2(\tau,\beta) - G_1(\tau,\beta))/G_2(\tau,\beta)$ between the Green functions obtained from ρ_1 and ρ_2.

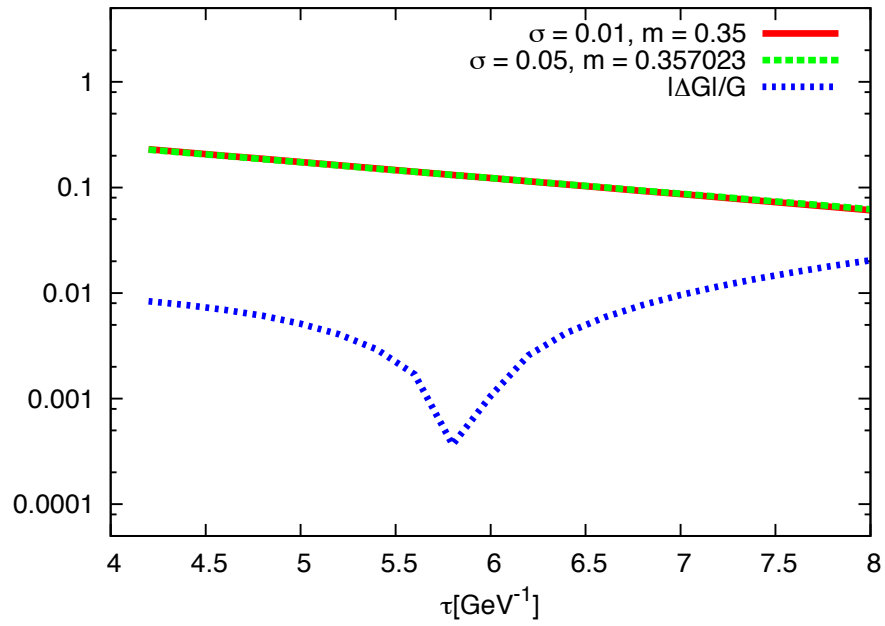

FIG. 4 (Color Online): $G_1(\tau)$, $G_2(\tau)$, and $|\Delta G|/G$, plotted together.

If $G(\tau)$ is determined with sufficient accuracy, deconvolution can be attempted. Again, the inverse Laplace transform is analytically easy but numerically non-trivial. Working with tens of data points for $G(\tau)$, no matter the accuracy, underdetermine any reasonable discretization of the spectral function. Consider χ^2-minimization in this situation: the spectral function is discretized into ~ 1000 points and ~ 10 data points are fitted, unnaturally small values of χ^2 can be achieved. The result for $\rho(\omega)$ usually appears choppy in this situation. The principle of maximum entropy suggests that the best fit for $\rho(\omega)$ is not the fit with the smallest χ^2, but the fit with a reasonable value for χ^2 but is also constrained by the information entropy

$$I = \sum_i \left[\rho_i \log\left(\rho_i/\sigma_i\right) - (\rho_i - \sigma_i)\right], \tag{7}$$

where ρ_i are the discretized values for $\rho(\omega)$ and σ_i are the *priors* for ρ_i. This constraint on the χ^2-minimization is often cast in terms of Bayesian principles, but it can also be thought of as an assumption of smoothness for the deconvolved function, far less controversial in physical situations. The sum of χ^2 and I define the energy function to be minimized:

$$E(\rho_i) = \chi^2(\rho_i) + \alpha I. \tag{8}$$

The coefficient α determines the relative importance of χ^2 and I in the minimization; it is often chosen to make χ^2 roughly equal the number of data points. Gallicchio and Berne point out that the best value for α can also be determined with Bayesian logic [15]. Our choices for α will be based simply on whether or not they yield reasonable values for χ^2.

A suitable algorithm for the minimization of this function is simulated annealing: 1.) random steps are considered in the space of values for ρ_i, , changing the value of E from E_i to E_f, 2.) any step that decreases E is taken while any step increasing E is taken with probability $P = \exp(-(E_f - E_i)/T)$, T being a temperature chosen to be large initially, and 3.) the process is repeated with T lowered until a minimum temperature T is reached. When a function is multi-modal as is possibly the case, simulated annealing is far more likely to be successful at finding absolute minima than the biconjugate gradient method, or any other slope-following method.

At this point, a test of this method of deconvolution would be useful. We can test this by going in the opposite direction: starting with a given spectral function, finding its Laplace transform (with random Gaussian error added), and deconvolving with the maximum en-

	α=0.01	α=0.1	α=1
1st peak	17.15%	14.84%	3.58%
2nd peak	22.85%	10.29%	4.65%

TABLE I: The discrepency between the true spectral function and the results of deconvolution shown in Fig. 5.

tropy method. The spectral function

$$\begin{aligned}\sigma(\omega) = 1.2(e^{-\frac{(\omega-0.33)^2}{2*0.0174^2}} - e^{-\frac{(\omega+0.33)^2}{2*0.0174^2}}) \\ + 0.2(e^{-\frac{(\omega-1)^2}{2*0.108^2}} - e^{-\frac{(\omega+1)^2}{2*0.108^2}})\end{aligned} \tag{9}$$

mimics the form that we expect for the quarkonium spectral function at finite temperature. The data set

$$G(\tau_i) = \int \sigma(\omega) e^{-\omega\tau} d\omega + \Delta G_i \tag{10}$$

contains 15 points ranging from $\tau = 0.5$ GeV^{-1} and $\tau = 9.6$ GeV^{-1}, and ΔG_i is random Gaussian noise with standard deviation 10^{-6} GeV. In Figure 5, the results of the maximum entropy method with different values of α are compared to the original spectral function. In Table 1, the error in the widths of the peaks in the spectral function are shown for the different values of α, showing agreement within a few percent when $\alpha = 1$.

The results from applying the maximum entropy method to the results for the quarkonium Green functions are shown in Figure 6. It has resolved what should be a Dirac delta function in the spectral function without dissipation down to a width of 0.25 GeV. The spatial diffusion coefficient $2\pi TD = 5$ corresponds with an increase of the width to 1 GeV, signifying the state having a lifetime of 0.197 fm/c. The results of the simulated annealing for 2πTD=∞ with different α values can be seen in Figure 7. It is observed that the results are not sensitive to the value of α over a considerable range.

We end this section by noting the physics behind the changes of the spectral function in Figure 6. First, the centroid of the ground state peak is shifted to high ω with increasing η. This suggests that the mean radius of the ground state increases, under the influence of momentum transfer from the medium. This could honestly have been seen rather quickly, by examining the slope of $G(\tau)$ in Figure 1. A far less trivial result from the maximum entropy method is the increasing width of the ground state peak, indicating a decrease of

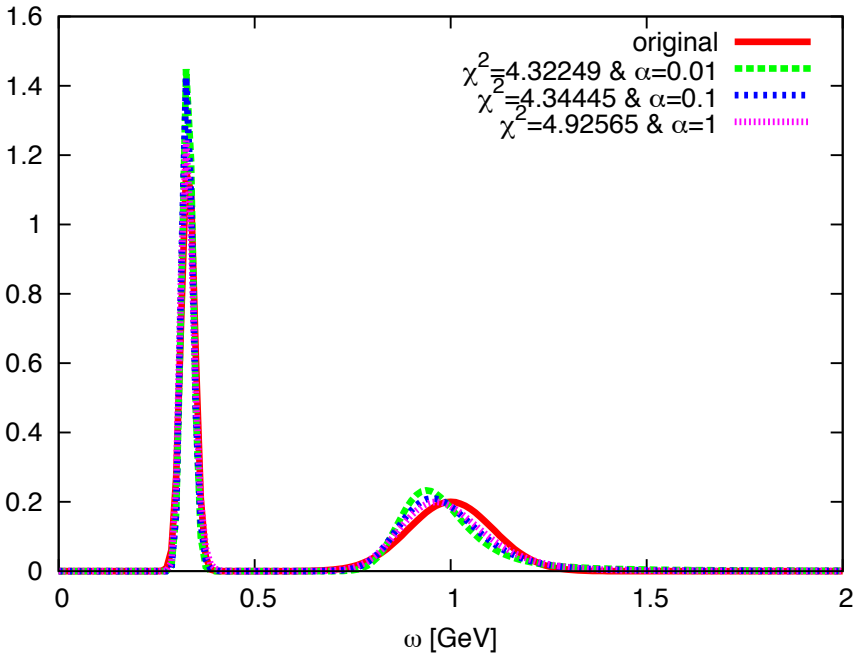

FIG. 5 (Color Online): The spectral functions deconvolved from the test data by using different values of α. The corresponding values of χ^2 are shown in the legend.

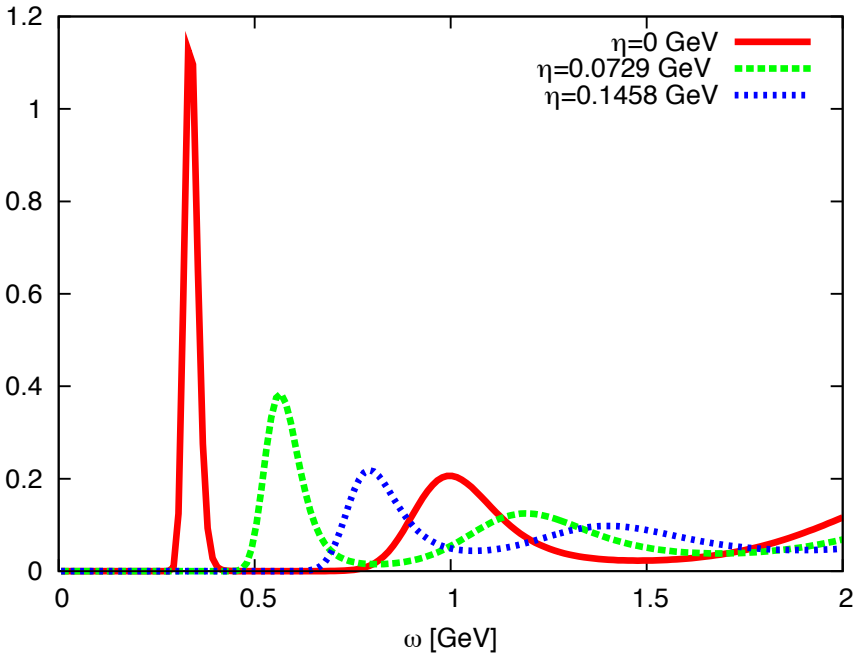

FIG. 6 (Color Online): The spectral functions deconvolved from the results in Figure 1. The corresponding values of χ^2 are shown in the legend.

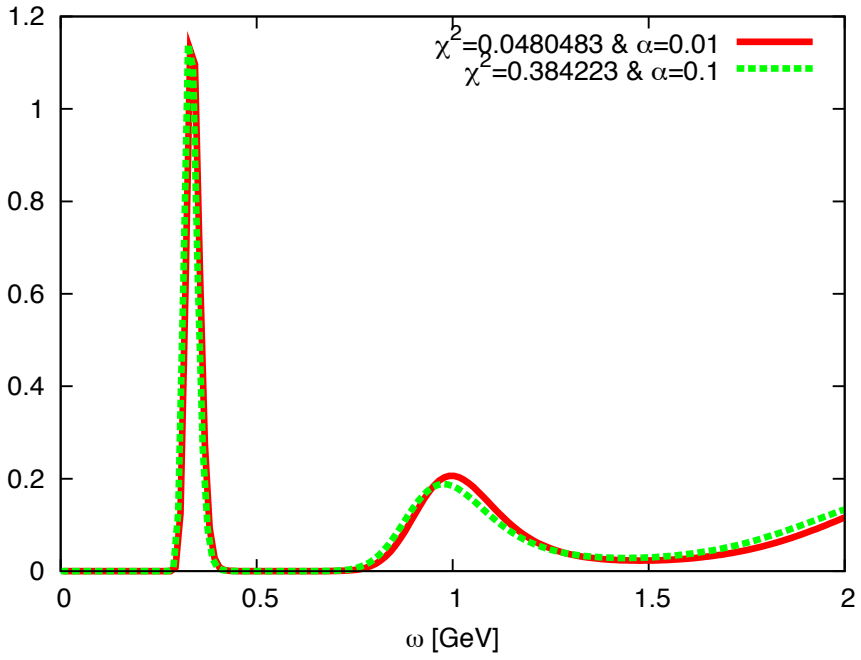

FIG. 7 (Color Online): The spectral functions deconvolved from the results where $\eta = 0$ in Figure 1 with different values of α. The corresponding values of χ^2 are shown in the legend.

the lifetime of the ground state.

IV. SUMMARY

Deconvolution of spectral functions was examined with an emphasis on the building of intuition for quarkonium near T_c. Results from a treatment of quarkonium above deconfinement as an open quantum system yielded a set of spectral functions showing the effect of increasing η, and these results were found to be robust for a range of values in α.

While this paper dug very deeply into the issues related to deconvolution, more work is required. In particular, only flat priors were used here; the role of the prior must be examined carefully. Finally, temperature-dependent potentials will be used in future work, making possible strong statements about quarkonium spectral functions including multiple temperature-dependent effects.

V. ACKNOWLEDGMENTS

This work was supported by the Natural Sciences and Engineering Research Council of Canada and by the U.S. DOE Grant No. DE-FG02-87ER40328. We especially thank Kevin Dusling for many important comments at the earliest stages of this work.

---

[1] N. Brambilla and A. Vairo, Nucl. Phys. Proc. Suppl. **74**, 201 (1999).

[2] N. Brambilla, M. A. Escobedo, J. Ghiglieri and A. Vairo, JHEP **1305**, 130 (2013).

[3] M. Laine, Nucl. Phys. A **820**, 25C (2009).

[4] C. Young and K. Dusling, Phys. Rev. C **87**, no. 6, 065206 (2013).

[5] A. Beraudo, J. P. Blaizot, P. Faccioli and G. Garberoglio, Nucl. Phys. A **846**, 104 (2010).

[6] Y. Akamatsu, Phys. Rev. D **91**, no. 5, 056002 (2015).

[7] Y. Akamatsu and A. Rothkopf, Phys. Rev. D **85**, 105011 (2012).

[8] C. Young and E. Shuryak, Phys. Rev. C **79**, 034907 (2009).

[9] C. Young, B. Schenke, S. Jeon and C. Gale, Phys. Rev. C **86**, 034905 (2012).

[10] Richard P. Feynman and A. R. HIbbs, *Quantum mechanics: the path-integral approach*, New York: McGraw-Hill (1965).

[11] A. O. Caldeira and A. J. Leggett, Physica **121A**, 587 (1983).

[12] H. Grabert, P. Schramm and G. L. Ingold, Phys. Rept. **168**, 115 (1988).

[13] D. M. Ceperley, Rev. Mod. Phys. **67**, 279 (1995).

[14] D. T. Son and D. Teaney, JHEP **0907**, 021 (2009).

[15] E. Gallicchio and B. J. Berne, J. Chem. Phys. **105**, 7064 (1996)